

REAL-TIME EARTHQUAKE DAMAGE DETECTION SYSTEM FOR BRIDGE STRUCTURES

Junichi Sakai¹, Hiroshi Kobayashi² and Shigeki Unjoh³

Abstract

When a large earthquake occurs, roads and bridges are fundamental infrastructure to evacuate the affected people and to transport the emergency equipment and materials. For these emergency activities, it is essential to detect immediately after the earthquake the severe structural damage that affects the capacity of structures. This paper proposes a method for the real-time earthquake damage detection/evaluation of reinforced concrete bridge columns. An intelligent sensor is developed that captures changes in the natural period of a bridge column. The applicability and efficiency of the proposed method was studied through a series of shake table tests of reinforced concrete bridge column models. The maximum response ductility estimated by the method provides good agreement with the actual ductility.

Introduction

When an extreme earthquake occurs, roads and bridges are fundamental infrastructure to evacuate the affected people and to transport the emergency equipment and materials. For these emergency activities, it is essential to evaluate the structural safety and operability of such structures immediately after the event. Thus, quick detection of severe damage that affects the structural safety is necessary to be done as soon as possible.

Currently, detection/evaluation of the degree of damage and structural safety of bridge structures is done by visual inspection of experts; however, there are various problems on this procedure, such as: the lack of uniform standards for quantitative evaluation of the degree of damage, the difficulty of visual inspection for underground/underwater structures, and the time-consuming process for gathering and analyzing the information with a limited number of personnel. Therefore, there is a strong need to develop a method for accurate and speedy determination of the degree of damage without experts' inspection.

For detecting and evaluating the seismic damage without visual inspections, the authors have been conducting a research project to develop a damage detection method using intelligent sensors. The authors focus on changes of natural period of reinforced concrete bridge columns due to seismic damage, and a method estimating response

¹ Research Engineer, Earthquake Engineering Research Team, Earthquake Disaster Prevention Research Group, Public Works Research Institute, Tsukuba, Japan

² Assistant Manager of Survey and Design Group, Osaka Business and Maintenance Department, Hanshin Expressway Company Limited, Osaka, Japan

³ Leader, Earthquake Engineering Research Team, Earthquake Disaster Prevention Research Group, Public Works Research Institute, Tsukuba, Japan

ductility of columns has been developed based on the results from a series of shake table tests for reinforced concrete bridge column models that failed in flexure at the bottom of the columns (Kobayashi & Unjoh 2004, Kobayashi et al. 2005).

In this paper, the efficiency of the proposed method is evaluated based on the results of additional series of shaking table tests. The applicability is also evaluated for a reinforced concrete bridge column that failed in shear.

Damage Detection System

Figure 1 shows a damage detection system proposed in this research project. The system is developed to be used for an emergency patrol after the big event by road administrators. The system contains an intelligent sensor unit that includes an accelerometer and a microcomputer, a relay box (if necessary), and a personal computer that indicates results. The key features of the system are:

- Ability for real-time damage detection
- Low cost for sensors and installation
- Easy handling of sensor units
- Emergency battery in case of electrical power failure due to earthquake

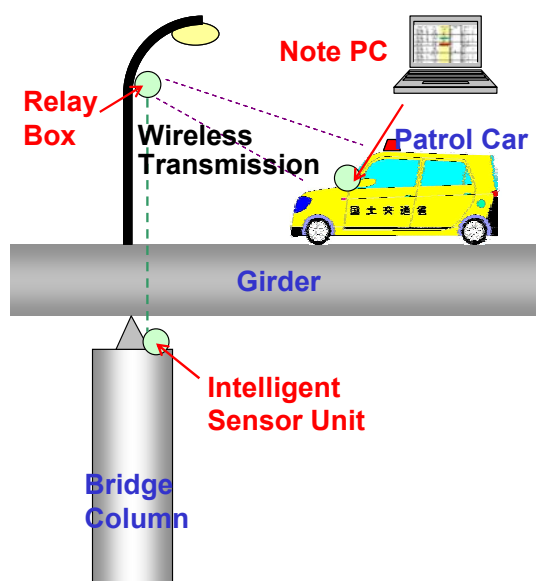


Figure 1 Damage detection system



Figure 2 Intelligent Sensor Unit

The intelligent sensor unit, shown in Figure 2, is placed on a column top to detect the change of natural period of the column, and the microcomputer calculates the estimated response ductility using the proposed algorithm, which will be described in the next chapter. The results are wirelessly transmitted from the intelligent sensor unit to the personal computer. If the signal condition is not good enough to transmit the results, however, a relay box is needed to help the transmission. This system enables

road administrators to gather information on the damage and safety of structures in a running patrol car during an emergency patrol.

Method Estimating Seismic Damage

This chapter introduces an outline of the proposed method (Kobayashi and Unjoh 2004, Kobayashi et al. 2005). The method is developed based on the results from a series of shake table tests of reinforced concrete bridge column models that fail in flexure at the bottom of the columns.

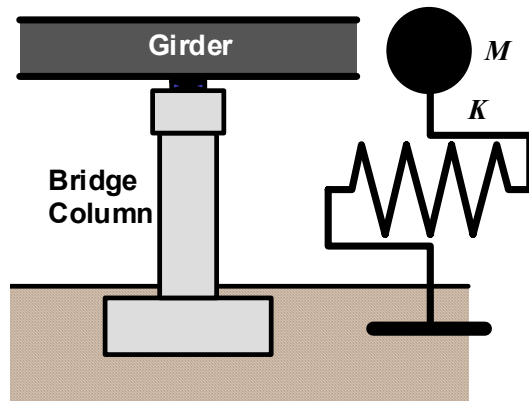


Figure 3 Idealization of bridge column

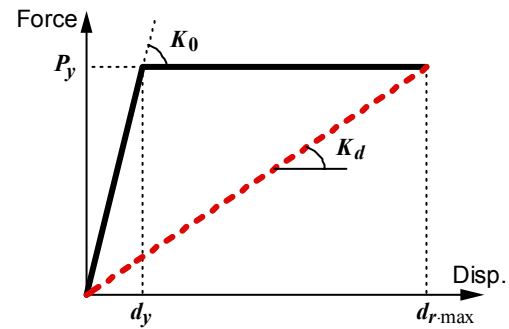


Figure 4 Elastoplastic skeleton curve

A bridge column is idealized as a single-degree-of-freedom (SDOF) system shown in Figure 3. The degree of seismic damage is estimated based on the change of natural period as follows.

The natural period T of the SDOF system is given as

$$T = 2\pi\sqrt{\frac{M}{K}} \quad (1)$$

where M and K are the mass and stiffness of the system, respectively. The change ratio of natural period before and after the damage is given as

$$\frac{T_d}{T_0} = \sqrt{\frac{K_0}{K_d}} \quad (2)$$

where T_0 and K_0 are the natural period and stiffness of the system before damage, and T_d and K_d are the natural period and stiffness of the damaged structure.

Assuming an elastoplastic skeleton curve of the restoring force versus deformation relation, as shown in Figure 4, the virgin stiffness, K_0 , is given as

$$K_0 = \frac{P_y}{d_y} \quad (3)$$

The damaged stiffness, K_d , is given as a secant stiffness of the point at the maximum response displacement $d_{r\cdot\max}$ for simplicity sake although K_d is dependent on the hysteretic characteristics of the structure.

$$K_d = \frac{P_y}{d_{r\cdot\max}} \quad (4)$$

By substituting Equations (3) and (4) for Equation (2), the maximum response displacement and ductility μ can be given as

$$\mu = \frac{d_{r\cdot\max}}{d_y} = \left(\frac{T_d}{T_0} \right)^2 \quad (5)$$

Because the maximum response ductility has strong correlation with the structural damage, the degree of damage can be estimated by the proposed method.

Efficiency of Method for Bridge Columns That Fail in Flexure

The efficiency of the proposed model is evaluated using the results from shake table tests of reinforced concrete bridge column models (Kobayashi & Unjoh 2004, Nishida and Unjoh 2004 & 2006, Sakai and Unjoh 2006). Table 1 summarizes the test considered in this study. Figure 5 shows cross sections of the specimens and test setup. The scale factor of the models was assumed to be about 4, and thus, the time of ground motions are scaled using a scale factor equal to 2 considering the similitude requirements of the specimen. The height from the bottom of the column to the center of gravity of the top mass is 3 m. All the specimens were designed to fail in flexure at the bottom of the column. Specimen 1 was tested under one horizontal ground motion, Specimen 3, 4 and 5 were tested under 2 horizontal ground motions, and Specimen 2 and 6 were tested under three directional (two horizontal and one vertical) ground motions.

For specimen 1, the amplitude of excitation was increased step-wisely. For the other specimens, each shake table test had two phases; one was for dynamic response in elastic range, and the other was for that in nonlinear range. Minor damage such as flexural cracks but no yielding of longitudinal reinforcement was observed during the elastic level test. Considerable damage (spalling of cover concrete, and buckling of longitudinal reinforcement, but no fracture of rebar as shown in Figure 6 (a)) was observed after the test for Specimen 1, 2, 3, 4 and 5. More severe damage such as fracture of longitudinal reinforcement occurred during the nonlinear level excitation for Specimen 6 as shown in Figure 6 (b). More details of the tests can be found in the references listed in Table 1.

Table 1 Specimens designed to fail in flexure

	Cross Section	Dimension	Reference
Specimen 1	Rectangular	800 × 450 mm	Kobayashi & Unjoh 2005
Specimen 2	Rectangular	800 × 450 mm	Nishida & Unjoh 2006 Kobayashi et al. 2005
Specimen 3	Square	600 × 600 mm	Nishida & Unjoh 2004
Specimen 4	Circular	ϕ 600 mm	
Specimen 5	Rectrangular	800 × 450 mm	
Specimen 6	Circular	ϕ 600 mm	Sakai & Unjoh 2006

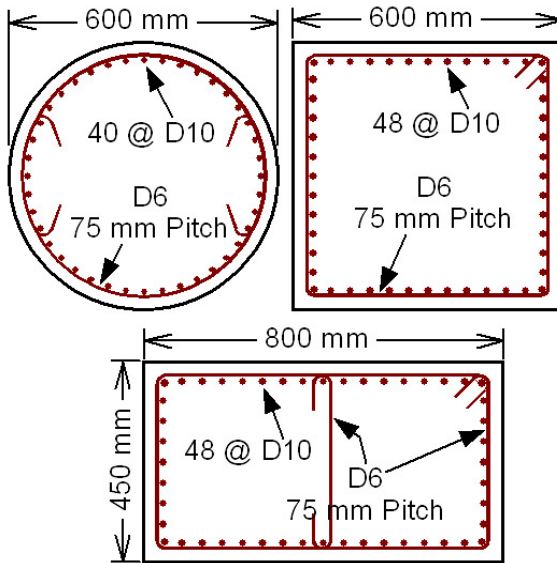


Figure 5 Cross sections of specimens



(a) Specimen 4



(b) Specimen 6

Figure 6 Failure modes

To evaluate the efficiency of the proposed method, the change of natural period was computed for each test. Figure 7 shows the time histories of the input ground motion, response acceleration and displacement at the center of gravity of the top mass, and the change of natural period that was computed by Fast Fourier Transform (FFT) of the response acceleration for the nonlinear tests of Specimens 3, 4 and 6. Three seconds is used for the computation period of FFT. Due to the seismic damage, the natural period elongates. The natural period has the trend that the value of the natural period increases as the response displacement increases, and then smaller values of the natural period are observed during the free vibration portion.

Figure 8 demonstrates the accuracy of the estimated response ductility by the method. Results of the column that fails in shear, which will be described later, are also shown in the figure. The estimated ductility due to the change of natural period is obtained from Equation (5). The natural period during the first 3 seconds in the elastic level test is used as the natural period before damage, T_0 , and those during free vibration portion (from 27 to 30 seconds for Specimens 1, 2, 3, 4 and 5 and from 57 to 60 seconds for Specimen 6) are used as the natural period after damage, T_d . To compute the actual response ductility, the maximum response displacement $d_{r,max}$ in

each principal direction is divided by the computed yield displacement, which is calculated according to the Japanese Design Specifications of Highway Bridges (Japan Road Association 2003). According to Figure 8, the estimated ductility provides a good agreement with the actual ductility, and thus, the method has ability to provide information about the structural damage.

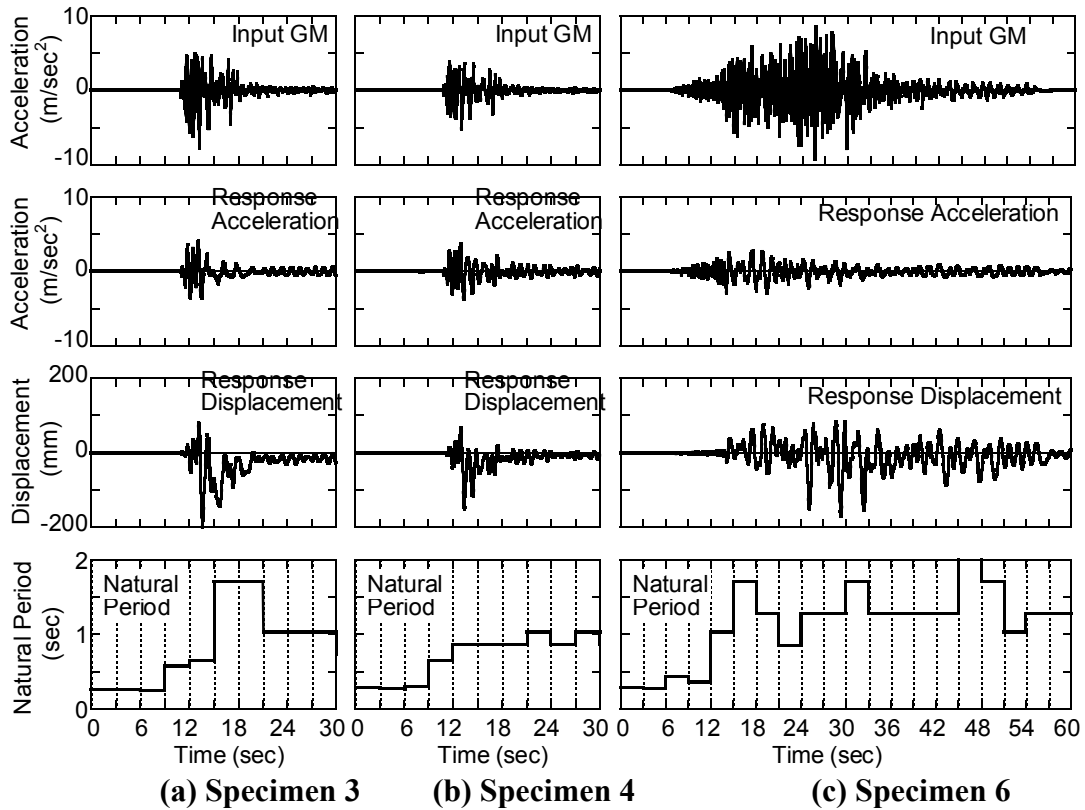


Figure 7 Response of specimens and change of natural period

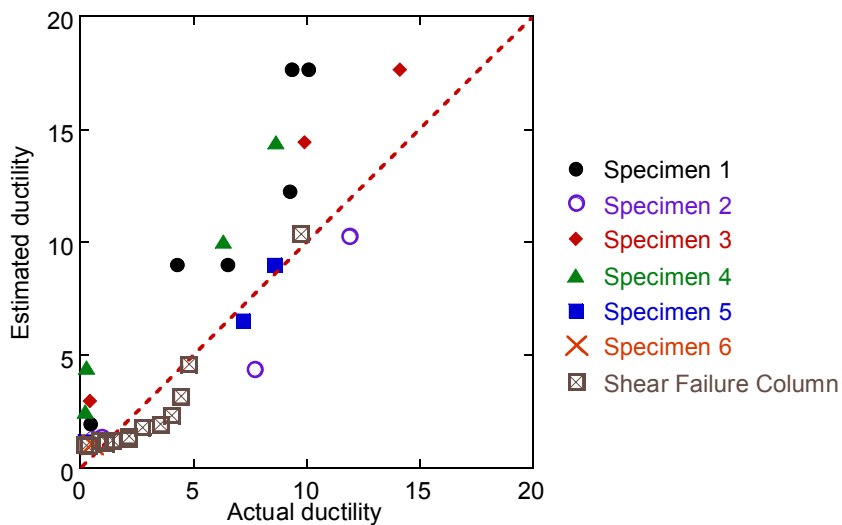


Figure 8 Efficiency of proposed method

Applicability of Method for Bridge Column That Fails in Shear

As described in the previous chapter, the proposed method has an ability to estimate the seismic damage of columns that fail in flexure. Because the damaged stiffness, K_d , is dependent on the hysteretic characteristics, however, it is necessary to evaluate the applicability for columns that has different type of hysteretic characteristics. Thus, a series of shake table tests for a bridge column model that fails in shear was conducted.

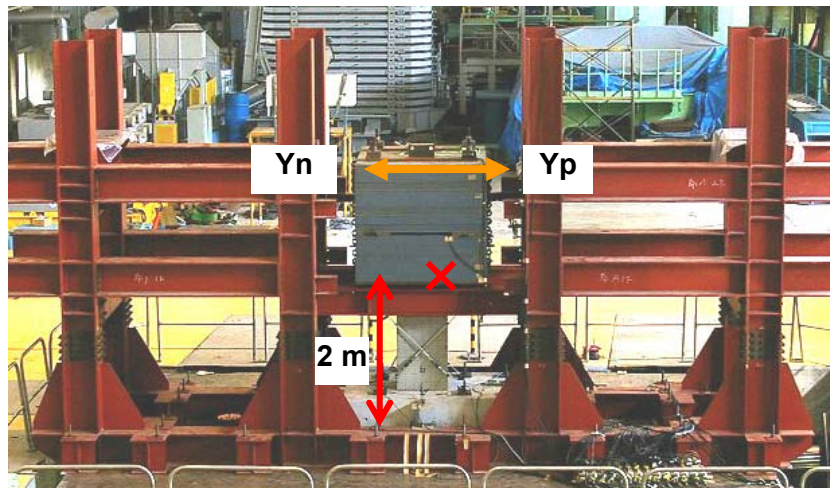
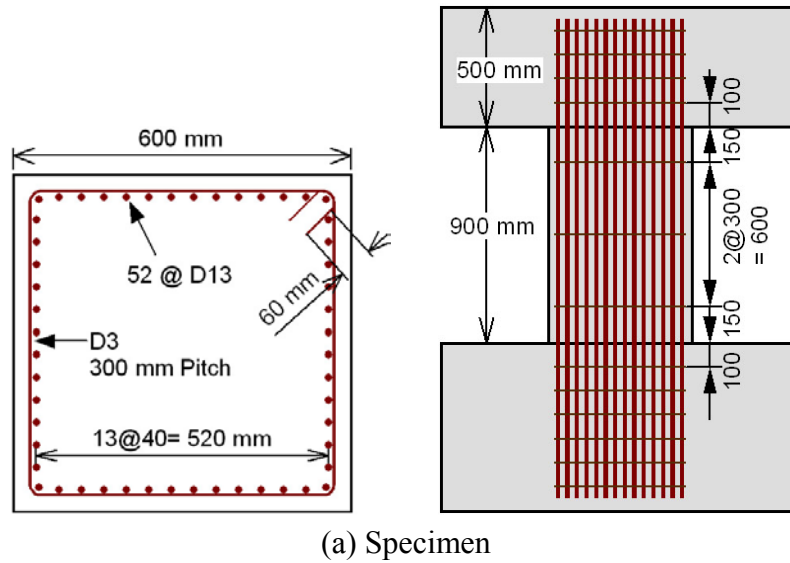


Figure 9 Specimen designed to fail in shear and test setup

Figure 9 shows the specimen tested in this study. This is a 1/4-scale model. The specimen had a 0.6×0.6 m-square cross section. The column height was 0.9 m, and the height from the bottom of the column to the center of gravity of the top mass was 2 m. The specimen supported steel plates that idealize the inertia mass and dead load from a superstructure as shown in Figure 9. The inertia mass was 35 ton and the axial stress

induced at the bottom of the column was 1 N/mm^2 . Design strength of concrete was 24 N/mm^2 , and the actual concrete strength on the test day was 22.5 N/mm^2 as shown in Table 2.

Table 2 Material properties

	Elastic Modulus	Strength f_{c0} or f_{sy}
Concrete	27.9 GPa	22.5 MPa
Longitudinal reinforcement	185.2 GPa	384.4 MPa
Shear reinforcement	140.0 GPa	306.8 MPa

The amount of longitudinal and transverse reinforcement was determined to have the specimen failed in shear. The specimen was reinforced longitudinally with 52 of 13-mm diameter deformed bars (D13), providing a longitudinal reinforcement ratio of 1.83%. For shear reinforcement, 3-mm diameter deformed bars (D3) was arranged at a 300-mm pitch. The D13 and D3 bars had yield strengths of 384 N/mm^2 and 307 N/mm^2 , as summarized in Table 2.

Assuming the actual material properties, the crack, first yield and ultimate flexural strength based on the JRA design specification (Japan Road Association 2003) are 56, 285 and 333 kN, respectively. The computed crack and first yield displacements are 0.4 and 5.9 mm, respectively. The shear capacity according to the JRA specification is calculated to be 177 kN, which is 62% and 53% of the first yield and ultimate flexural strength. If the allowable shear stress is given from Equation (6) (Kawano et al. 1996), the shear capacity is estimated to be 275 kN, which is 3.5% smaller than the first yield flexural strength.

$$\tau_c = 0.72 \times d^{-0.33} \times \left(\frac{24}{f_{c0}} \right)^{-1/3} \times \left(\frac{1.2}{p_t} \right)^{-1/3} \quad (6)$$

The specimen was tested under one directional ground motion. The North-South component of the ground motion records observed at the JR Takatori station during the 1995 Hyogo-ken Nanbu, Japan, earthquake (Nakamura 1995) was inputted to the Y direction as shown in Figure 9. The sides face the Y positive and the Y negative directions are defined as the Yp and Yn faces, respectively. Likewise, the Xp and Xn faces are defined.

Time of the input signal was scaled with a scale factor of 2, and the amplitude of the ground motion was step-wisely increased by 10% from 10% of the original intensity of the signal as shown in Table 3. White noise was inputted to the shake table prior to each test to investigate the dynamic properties and change of natural period of the specimen.

Table 3 summarizes the maximum response force and displacement, and observed damage. The natural periods prior to the test in Table 3 are obtained from the white noise test. Figure 10 shows the input ground motion, response acceleration and

displacement, change of natural period, and force-displacement hysteresees for 60%-2nd, 100% and 120% tests. Figure 11 shows the damage progress. The lateral force is computed from the multiplication of the inertia mass and the response acceleration. During 50% and 60% tests, the steel plates slipped during the excitation; thus, these tests were redone after the steel plates were tied firmly.

Table 3 Response and damage progress of specimen that failed in shear

	Natural Prieod (sec)	Respons e Disp. (mm)	Lateral Force (kN)	Damage Observed
10% Test	0.16	0.9	54	No crack
20% Test	0.16	1.9	104	No crack
30% Test	0.16	5.6	180	Few flexural cracks at Yp, Yn faces
40% Test	0.17	8.0	215	
50% Test	0.17	9.9	230	
60% Test	0.18	15.0	236	Diagonal cracks at Xp, Xn faces
50%-2 Test	0.17	14.8	302	Progress of diagonal cracks Yielding of longitudinal reinforcement
60%-2 Test	0.18	18.9	330	Progress of diagonal cracks
70% Test	0.20	24.4	341	Progress of diagonal cracks; Crack width = 0.06 mm
80% Test	0.21	27.9	348	Progress of diagonal cracks; Crack width = 0.15 mm
90% Test	0.23	30.7	350	Progress of diagonal cracks; Crack width = 0.35 mm
100% Test	0.27	33.1	345	Minor crush of cover concrete at Yp, Yn faces Progress of diagonal cracks; Crack width = 0.55 mm
120% Test	0.32	67.3	360	Shear failure

During 30% tests, few flexural cracks were observed on the Yp and Yn faces. The maximum response lateral force during this test was 180 kN, which was larger than the crack strength, but still smaller than the first yield flexural strength and shear capacity obtained from Equation (6). As the intensity of the ground motion increased, the flexural cracks progressed, but no shear crack was observed up to 50%-2nd test. During this test, the lateral force exceeded the first yield strength and shear capacity, and yielding of the longitudinal reinforcement occurred. After this test, shear cracks progressed. After the 100% test, the maximum width of the cracks increased up to 0.55 mm. And then the specimen failed in shear during 120% test. The cover concrete spalled and longitudinal reinforcement were buckled at the Yn face, and shear reinforcement were fractured as shown in Figure 11.

As shown in Table 3 and Figure 10, the natural period increased as the damage progressed. In Figure 8, the applicability of the proposed method to estimate the damage of the column that fails in shear is shown. The figure demonstrates that the estimated ductility increases as the damage progresses. For the 120% test, the estimated ductility is 10.4, which is close to the measured ductility (= 9.8). As a whole, the proposed method can provide a good estimation of the response ductility of the column.

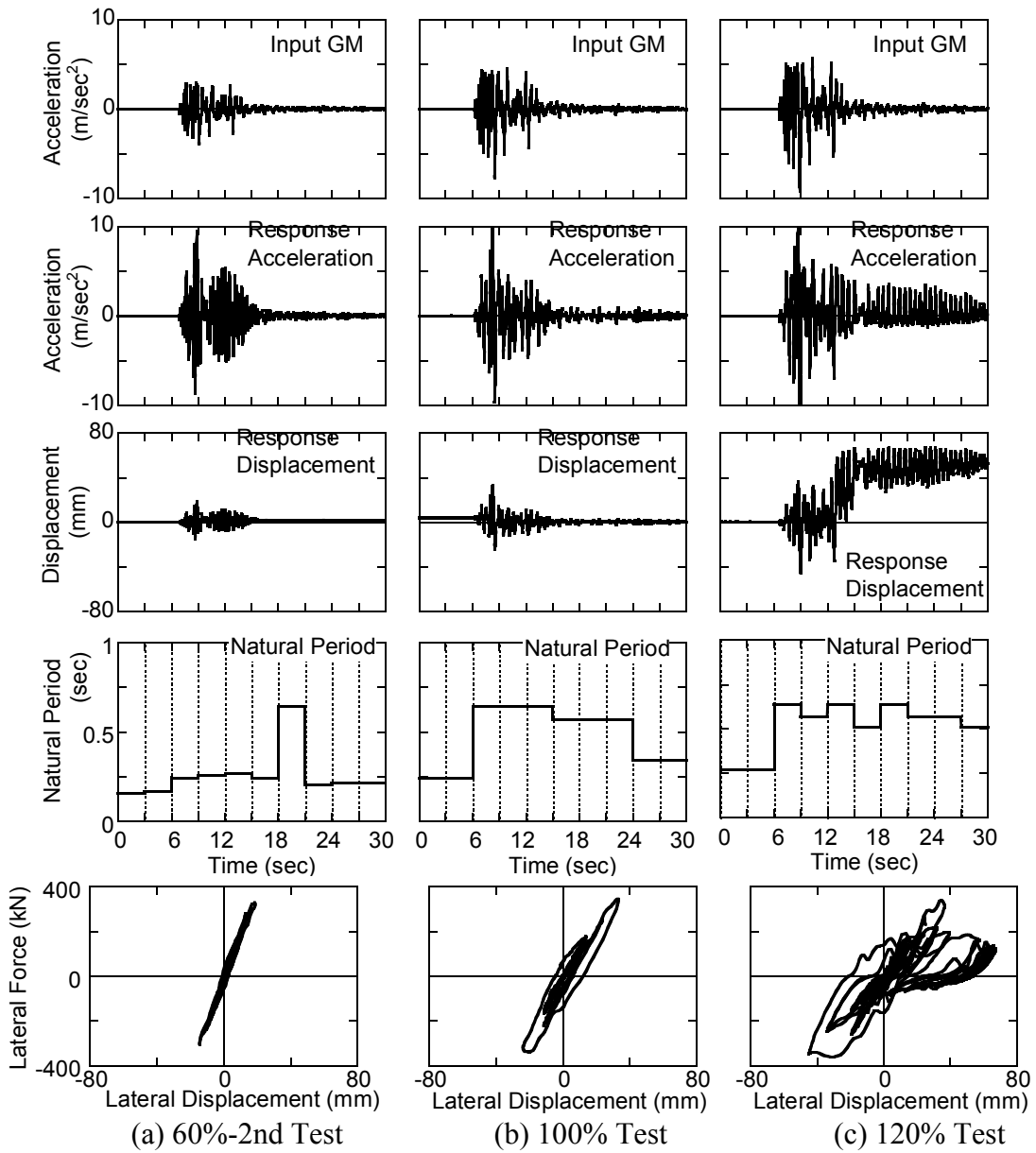


Figure 10 Response of specimen that failed in shear

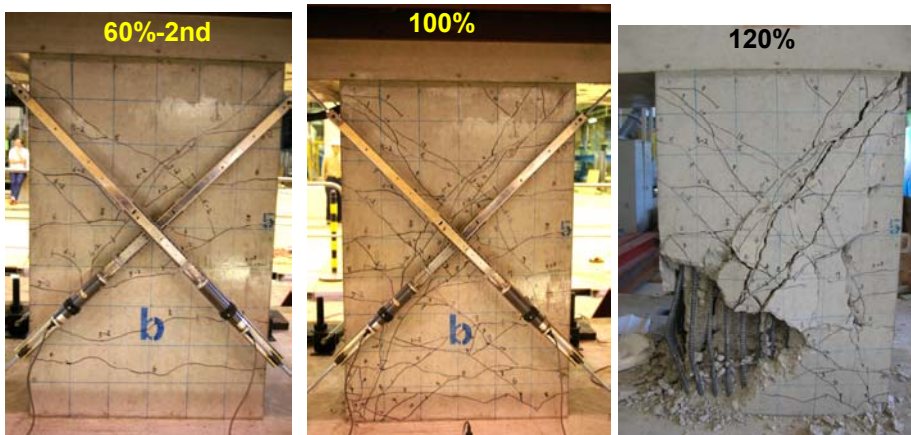


Figure 11 Damage progress

Conclusions

To develop a quick detection system of seismic damage for bridge structures, a method estimating seismic damage of reinforced concrete bridge columns based on the change of natural period is proposed, and the accuracy of the method is evaluated with the results of shake table tests for bridge column models. Below are the conclusions determined from the study:

1. The natural period of reinforced concrete columns elongates due to seismic damage. The natural period has the trend that the maximum value of the natural period occurs at around the maximum response displacement.
2. Estimated ductility of the columns that fail in flexure at the bottom of the columns provides a good agreement with the actual ductility.
3. The proposed method also provides good estimation of shear damage of reinforced concrete bridge columns.

References

Japan Road Association (2003). *Specifications for highway bridges. Part V Seismic design*, Japan.

Kawano, H., Watanabe, H. and Kikumori, Y. (1996). "Report on shear strength of large scale reinforced concrete beams." *PWRI Technical Memorandum*, Public Works Research Institute, No. 3426, Japan. (in Japanese)

Kobayashi, H. and Unjoh, S. (2004). "Development of an earthquake damage detection system for bridge structures." *Proc. of 20th US-Japan Bridge Engineering Workshop*, pp. 125-132, Washington D.C., USA.

Kobayashi, H., Unjoh, S. & Kanoh, T. (2005). "Development of an earthquake damage detection method for bridge structures with the accelerating sensor." *Journal of Earthquake Engineering*, JSCE, Vol. 28, CD-ROM No. 23. (in Japanese)

Nakamura, Y. (1995). "Waveform and its analysis of the 1995 Hyogo-ken Nanbu earthquake." *JR Earthquake Information*, Railway Technical Research Institute, No. 23c Japan.

Nishida, H. and Unjoh, S. (2004). "Dynamic response characteristic of reinforced concrete column subjected to bilateral earthquake ground motions." *Proc. of 13th World Conference on Earthquake Engineering*, CD-ROM No. 576. Vancouver, Canada.

Nishida, H. and Unjoh, S. (2006). "Shake table test of rectangular reinforced concrete column." *Proc. of 9th Symposium on Ductility Design Method for Bridges*, JSCE, pp.327-330. Tokyo, Japan. (in Japanese)

Sakai, J. & Unjoh, S. (2006). "Earthquake simulation test of circular reinforced concrete bridge column under multidirectional seismic excitation." *Earthquake Engineering and Engineering Vibration*, Vol. 5, No. 1, pp.103-110.